Molecular-dynamics simulation of electron-irradiation-induced amorphization of $NiZr_2$

R. Devanathan*
Materials Science Division, Argonne National Laboratory, Argonne, Illinois 60439
and Department of Materials Science and Engineering, Northwestern University, Evanston, Illinois 60208

N. Q. Lam and P. R. Okamoto
Materials Science Division, Argonne National Laboratory, Argonne, Illinois 60439

M. Meshii
Department of Materials Science and Engineering, Northwestern University, Evanston, Illinois 60208
(Received 8 February 1993)

We have used molecular-dynamics simulations to examine electron-irradiation-induced amorphization of the ordered intermetallic compound $NiZr_2$. The principal effects of irradiation by MeV electrons, namely chemical disorder and Frenkel-pair generation, were simulated in two separate processes: Chemical disorder was created by exchanging randomly selected Ni and Zr atoms, and Frenkel pairs were introduced by removing atoms at random from their sites and introducing them into interstitial positions. The interactions between the atoms were governed by embedded-atom potentials. During the simulation, the potential energy, volume, radial distribution function, elastic constants, and mean-square atomic displacement were calculated as functions of damage dose. In addition, the structure of the system was characterized by diffraction patterns obtained with the use of the multislice method in conjunction with the simulation. Our results indicate that both random atom exchanges and Frenkel-pair introduction can amorphize $NiZr_2$. At the critical dose of about 0.16 dpa (displacements per atom), the energy and volume attained values corresponding to the quenched liquid and the system became elastically isotropic. Moreover, the variation of the average shear elastic constant with mean-square atomic displacement, following isothermal disorder and isobaric heating, provides evidence in favor of a unified description of amorphization and melting. The results obtained in the present work are in agreement with experimental observations.

I. INTRODUCTION

Amorphous metallic alloys can be produced by rapid quenching from the melt, electrodeposition, vapor deposition, sputtering, or by a variety of solid-state amorphization techniques.[1] These techniques include irradiation by energetic particles, mechanical alloying, annealing of multilayer films, and hydrogenation. Solid-state amorphization has gained considerable interest in recent years because of the inherent limitations of conventional glass-forming methods, such as melt quenching. Amorphization by quenching requires cooling rates in excess of 10^6 K/s. The necessity of attaining such high rates throughout the material restricts this process to thicknesses of the order of 100 μm. On the other hand, it is possible to amorphize bulk crystalline alloys in the solid state. Of the known solid-state techniques, electron-irradiation-induced amorphization has been most extensively studied[2–9] for several reasons. First, the damage produced by electron irradiation is simple to study, because it consists merely of chemical disorder and Frenkel pairs. Since the energy transferred by a 1-MeV electron to the crystal is such that only one or two atoms are displaced from their lattice sites, phenomena such as cascades and thermal spikes need not be considered. Second, amorphization by electron irradiation has features which are generally representative of solid-state amorphization. Third, it is possible to introduce damage in a controlled manner and study the effects *in situ* in a high-voltage electron microscope (HVEM). By carrying out the irradiation in a HVEM, the changes in the structure of the specimen can be readily analyzed using a variety of electron-microscopy techniques.

Several HVEM experiments have been performed to understand the mechanism of the transformation. The relative importance of chemical disorder and Frenkel pairs in causing amorphization has, however, remained unresolved. One of the earliest observations of electron-irradiation-induced amorphization was made by Carpenter and Schulson,[2] who irradiated the $L1_2$ compound Zr_3Al with 1-MeV electrons in the temperature range 130–775 K. They observed diffuseness in dislocation lines along with the appearance of diffuse rings in the diffraction pattern after a dose of about 1 dpa at 130 K. However, the crystalline spots did not disappear, indicating the occurrence of partial amorphization at dislocations. Similar observations have been made by Mori, Fujita, and Fujita,[3,4] who studied the effects of 2-MeV electron irradiation on the $B2$ compound NiTi. They observed the formation of small amorphous islands along dislocation lines and concluded that the concentration and mobility of points defects produced by electron irra-

0163-1829/93/48(1)/42(10)/$06.00

diation play an essential role in the observed transition. Since vacancy enrichment occurs around dislocations due to the preferential annihilation of interstitials, the authors proposed that amorphization occurs by the accumulation of vacancies in excess of a critical concentration. Pedraza[5] has modeled the amorphization kinetics in NiTi based on the accumulation of vacancy-interstitial complexes, which are stabilized by chemical short-range order. A complex binding energy of 0.7–1.0 eV was assumed to fit the results of Mori and Fujita.[3] The role of vacancies in the transformation has, however, been questioned by Limoge and Barbu.[6] They have stated that the strong effect of the interstitials on the elastic constants probably provides the lattice softening accompanying amorphization. The role of point defects in bringing about amorphization has also been pointed out by Koike *et al.*[7] following their observation of diffuse scattering in diffraction patterns, and striations in bright-field images of Zr_3Al irradiated with 1-MeV electrons at 57 K.

In contrast to these studies, Luzzi *et al.*[8,9] have brought forth evidence in favor of chemical disorder as the dominant form of energy storage in the lattice. The authors systematically examined the changes in the structure of Cu_4Ti_3 following irradiation with 2-MeV electrons in the temperature range 175–315 K. They characterized the system by observing the changes in the diffraction pattern and the Bragg-Williams long-range-order parameter with electron dose, and by performing a high-resolution electron-microscopy (HREM) study of the crystalline-amorphous interface. At about 265 K, they observed a remarkable coincidence of the critical temperatures for amorphization and chemical disorder. Below this temperature, electron irradiation of Cu_4Ti_3 led to considerable chemical disorder and amorphization. Above 265 K, the compound retained a high degree of order and remained crystalline. Moreover, through their HREM studies, the authors found that the crystal cannot exist with complete chemical disorder. Based on the above evidence, Luzzi *et al.*[8] have concluded that chemical disorder increases the energy of crystalline Cu_4Ti_3 until it becomes unstable with respect to the amorphous state.

Despite the advances made in these *in situ* studies, it is impossible to separate the effects of Frenkel pairs from those of chemical disorder in a HVEM experiment, because they always occur together. This disadvantage can be overcome by performing a computer simulation of radiation damage. In a simulation, one can study the effects of various levels of chemical disorder and displacement damage in isolation. In spite of this potential advantage, most simulations of radiation effects have restricted their scope to pure elements because of the lack of reliable interatomic potentials for alloy systems. Massobrio, Pontikis, and Martin[10] have shown in a molecular-dynamics (MD) study with tight-binding potentials that chemical disorder can lead to amorphization in $NiZr_2$. This study did not examine the effects of Frenkel pairs on $NiZr_2$. On the other hand, Sabochick and Lam[11,12] have developed embedded-atom potentials for the Cu-Ti and Ni-Ti systems. Using these potentials, they have performed a MD simulation study of the relative importance of chemical disorder and Frenkel pairs in the amorphization of the compounds CuTi, $CuTi_2$, Cu_4Ti_3, Cu_4Ti, and NiTi.[11–13] Their results indicate that Frenkel pairs are required to amorphize these compounds, while chemical disorder, merely, increases the energy of the system without causing amorphization.

Recently, in an effort to improve our understanding of the driving force for solid-state amorphization, we have developed embedded-atom potentials for the Ni-Zr system.[14,15] The parameters of the potentials were fitted to the properties of the pure elements Ni and Zr, and three intermetallic compounds, viz., NiZr, $NiZr_2$, and Ni_3Zr. The Ni-Zr system was chosen to coordinate the simulation with the HVEM experiments of Xu *et al.*[16] on this system. These authors irradiated NiZr, $NiZr_2$, and Ni_3Zr with 1-MeV electrons in the temperature range 10–200 K and were able to completely amorphize all three compounds. In a previous study,[14,15] we had used our embedded-atom potentials to examine the effects of chemical disorder and the introduction of Frenkel pairs in NiZr. Our results indicated that both these processes can amorphize the compound and exhibited general agreement with the findings of Xu *et al.*[16] In the present report, we present our results from a MD simulation of electron-irradiation-induced amorphization of the intermetallic compound $NiZr_2$.

II. SIMULATION DETAILS

The present study employed constant-temperature, constant-pressure molecular-dynamics simulations using a vectorized version of the computer code DYNAMO.[17] The model lattice, representing $NiZr_2$ in the $C16$ structure, is shown in Fig. 1. The simulation cell was rectangular and contained 256 atoms of Ni and 512 atoms of Zr. A time increment of 2×10^{-15} s was used throughout the simulation. The interactions between the atoms were modeled by appropriate potentials developed using the approach of Oh and Johnson[18] on the basis of the embedded-atom method.[19] In order to facilitate a realistic comparison of our results with experimental observations, the parameters of the potentials were fitted to the lattice constants, elastic constants, and relaxed vacancy-formation energy of Ni and Zr, and the lattice constants and heats of formation of the compounds NiZr, $NiZr_2$, and Ni_3Zr. The details of the fit are given elsewhere.[14]

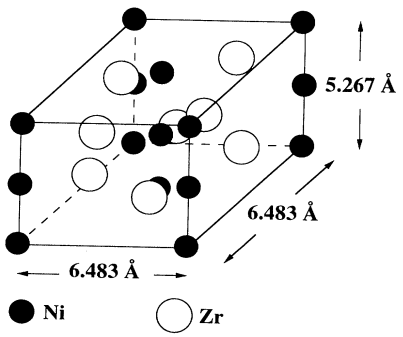

FIG. 1. Ordered structure of the compound $NiZr_2$.

The ability of our potentials to model the thermodynamic properties of $NiZr_2$ was examined by studying the melting of a perfect model crystal as well as a crystal containing an internal void. A perfect lattice was relaxed at various temperatures, and the properties of the system such as the energy, volume, and mean-square displacement were calculated as averages over 20 000 steps. Figure 2 shows the potential energy per atom E/N, volume per atom V/N, and the mean-square amplitude of thermal vibrations $\langle \mu^2_{\rm vib} \rangle$ as functions of temperature. At each temperature, the steady-state value of $\langle \mu^2_{\rm vib} \rangle$ was obtained from the expression

$$\langle \mu^2_{\rm vib} \rangle = \lim_{t \to \infty} \left\langle \frac{1}{N} \sum_{i=1}^{N} [r_i(t+t_0) - r_i(t_0)]^2 \right\rangle_{t_0} , \quad (1)$$

where r_i refers to the position of atom i, N is the total number of atoms in the system, and the angular brackets indicate an average over a set of values for the initial time t_0.

It can be seen from Fig. 2 that the energy and volume of the perfect crystal increase smoothly up to 1500 K, where an abrupt increase occurs. At 1525 K, $\langle \mu^2_{\rm vib} \rangle$ exhibited values characteristic of a liquid and the diffusion coefficient was calculated to be of the order of 10^{-5} cm^2/s. This indicates that our perfect model crystal, lacking surfaces and internal defects, melts between 1500 and 1525 K. From the variation of the volume with temperature, one can deduce a value of about 2×10^{-5} K^{-1} for the coefficient of linear thermal expansion. This is almost identical to the value reported by Massobrio, Pontikis, and Martin[10] and is in good agreement with the experimental results of Eshelman and Smith,[20] who estimated it to be of the order of 10^{-5} K^{-1}. The melting point of a crystal with a rectangular void was determined after removing 6 Ni and 12 Zr atoms from the center of the cell. The Ni and Zr atoms were removed in the ratio 1:2 to preserve stoichiometry. The changes in E/N and V/N with temperature for this case are shown by dashed lines in Fig. 2. The figure indicates that the crystal melts between 1300 and 1350 K when a void is introduced. This is in good agreement with the experimentally determined melting temperature of 1393 K (Ref. 21) shown by the arrow. In the liquid state, there is little difference between the energy and volume per atom of the perfect crystal, and the corresponding values of the crystal with a void. These results provide evidence in support of the reliability of our embedded-atom potentials.

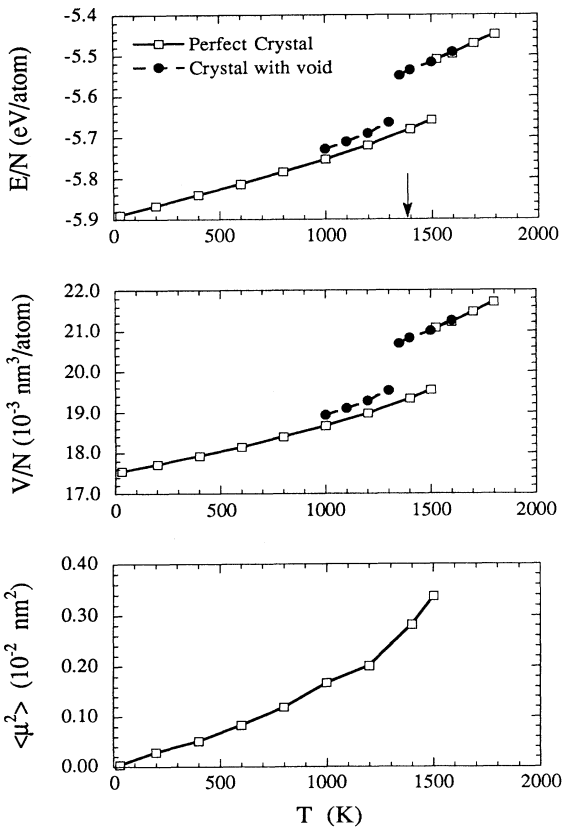

FIG. 2. Changes in the potential energy per atom, E/N, the volume per atom, V/N, and the mean-square amplitude of thermal vibrations, $\langle \mu^2_{\rm vib} \rangle$, as functions of temperature for the perfect crystal and a crystal with a void. The experimentally determined melting point is indicated by the arrow.

Following the determination of the melting point, the effects of electron irradiation were simulated as follows. The perfect lattice was maintained in equilibrium for 5000 time steps. Then, in separate runs, chemical disorder was introduced by exchanging a randomly chosen pair of Ni and Zr atoms every 10 time steps, and Frenkel pairs were created by removing a randomly selected atom and introducing it at a random interstitial site every 10 steps. During the introduction of Frenkel pairs, the atoms were maintained at a minimum separation of 0.07 nm to avoid numerical instabilities. The configurations corresponding to various damage doses were saved for further analysis. The dose is defined in terms of exchanges per atom (epa) for chemical disorder and displacements per atom (dpa) for Frenkel pairs.

The saved configurations were subsequently relaxed, and the thermodynamic, structural, and mechanical properties were determined as averages over 20 000 time steps. The structure of the system was characterized by calculating the [001] electron-diffraction patterns for various doses. The configurations from the MD simulations were used as input for the multislice method.[22,23] The simulation cell was divided into a number of slices perpendicular to the electron beam. In each slice the incident electron wave was multiplied by a phase grating, subjected to a Fourier transform, multiplied by a Fresnel propagator, and inverse Fourier transformed to get the wave at the bottom of the slice as shown in Fig. 3. The wave leaving the first slice was used as the incident wave for the next slice, and the process was repeated to obtain the wave at the bottom of the cell and hence the diffraction pattern. The complete details of this approach can be found elsewhere.[22–26] For the purpose of comparison, the properties of the quenched liquid were also calculated. This task was accomplished by equilibrating the system at 4000 K for 10 000 steps, quenching it to 30 K, relaxing it at 30 K, and finally calculating the properties as averages over 10 000 time steps.

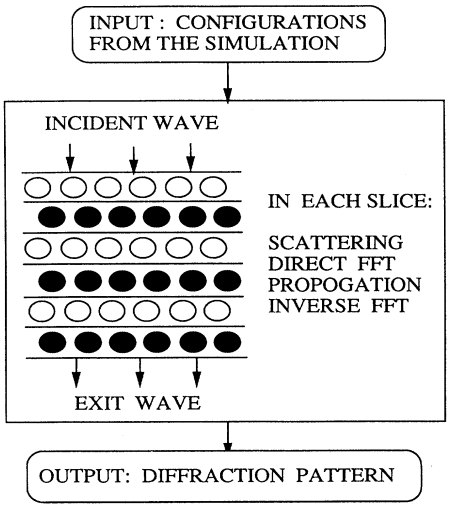

FIG. 3. Illustration of the approach to calculate diffraction patterns from simulated configurations.

III. RESULTS AND DISCUSSION

A. Thermodynamic properties

The energy and volume of the system are the easiest properties to determine in a MD simulation. Figure 4 shows, as functions of dose, the changes in the potential-energy increase per atom ($\Delta E/N$) and volume expansion ($\Delta V/V$) over the values of the perfect crystal. It is interesting to note that the volume varies with dose in a manner remarkably similar to the energy. In an irradiation experiment, the volume change can be measured easily as a function of dose. However, the determination of the variation of energy with dose is not straightforward. Our results indicate that the volume change can be taken as a measure of the energy change in such experiments. Both these quantities increase monotonically with dose until they reach the corresponding levels of a quenched liquid at about 0.16 dpa for Frenkel pairs and about 0.16 epa for exchanges. At higher doses, the energy and volume show very little further increase. The energy increase saturates at about 0.1 eV/atom above the perfect crystal, while the volume expansion reaches a saturation value of about 6.4%. Massobrio, Pontikis, and Martin[10] have reported that the volume expansion corresponding to amorphization in $NiZr_2$ was about 2%. Our value of 6.4% is closer to the experimental result of Xu *et al.*,[16] who observed a volume expansion of 5.4% following 1-MeV electron irradiation of $NiZr_2$. The behavior of the energy and volume suggests that both atom exchanges and Frenkel-pair introduction might be able to amorphize $NiZr_2$. However, it has been shown in NiTi by Sabochick and Lam[12] that the attainment of the quenched liquid level by the energy and volume is not necessarily a sign of amorphization. The structural properties are better indicators of amorphization than the thermodynamic properties.

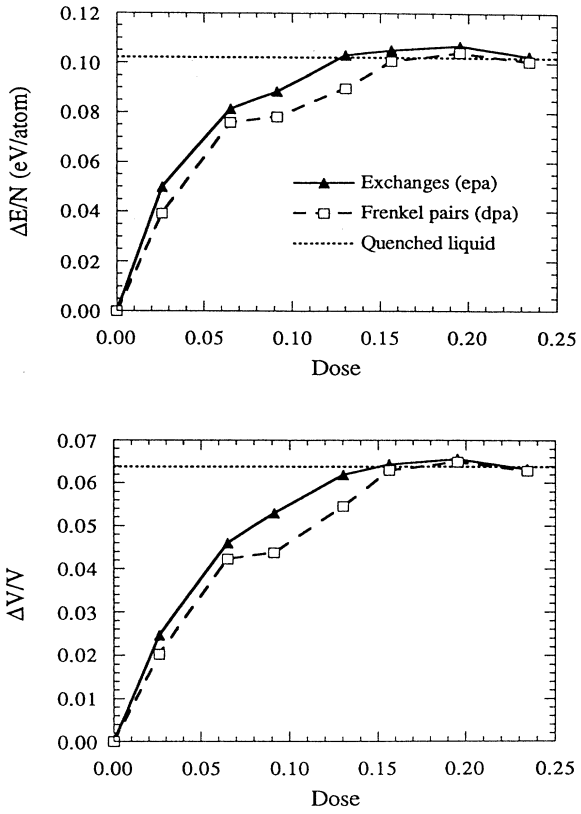

FIG. 4. Variation of the potential energy increase per atom, $\Delta E/N$, and the volume expansion $\Delta V/V$ with damage dose. The dotted lines represent the values corresponding to a quenched liquid.

B. Structural properties

The structure of the system was characterized by the pair-correlation function $g(r)$, long-range-order parameter S, calculated [001] electron-diffraction patterns, and projections of atom positions along the [001] direction. Figure 5 shows the global $g(r)$ of $NiZr_2$ corresponding to various doses. For doses of 0.09 epa and 0.16 dpa $g(r)$ resembles that of the quenched liquid. The Ni-Ni, Zr-Zr, and Ni-Zr partial $g(r)$ (not shown here) were also calculated. The changes in these functions were similar to those in the global $g(r)$. Although $g(r)$ indicates the occurrence of amorphization with exchanges as well as Frenkel pairs, one has to be cautious in interpreting this data. It has been pointed out in the literature[12,22] that $g(r)$ is not sensitive to the structural changes accompanying amorphization. In particular, Sabochick and Lam[12] have shown, in the case of NiTi, that $g(r)$ may show amorphous characteristics even when the material is crystalline. The structure factor or the calculated diffraction pattern is considered a more reliable indicator of the structure of the system. Moreover, the experimental definition of amorphization is based on the appearance of an amorphous halo in the diffraction pattern. By obtaining the diffraction pattern in a simulation, one can make a direct comparison with experiments.

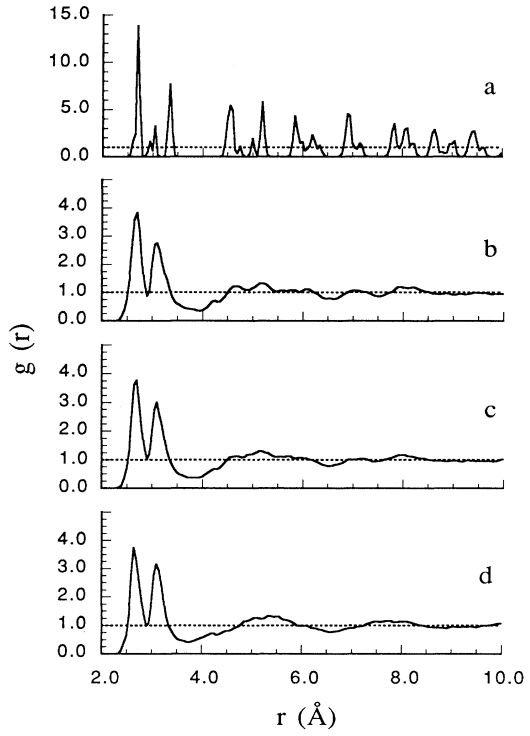

FIG. 5. Global pair-correlation function for the following configurations: (a) perfect crystal, (b) 0.09 epa, (c) 0.16 dpa, and (d) quenched liquid.

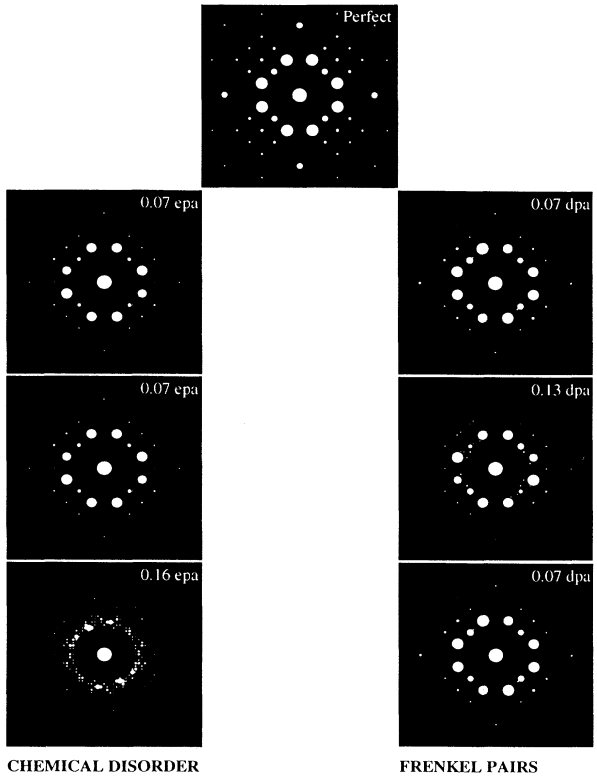

FIG. 6. [001] electron-diffraction patterns calculated for various doses as indicated.

The calculated [001] diffraction patterns are shown in Fig. 6 for various doses as indicated on the top right corner. The column of patterns on the right is for Frenkel-pair introduction, while that on the left is for chemical disorder. It is interesting to note that the diffraction pattern corresponding to 0.09 epa clearly shows crystalline features (diffraction spots), while $g(r)$ at this dose resembles that of a quenched liquid. Since the energy and volume do not attain saturation values for a dose of 0.09 epa (Fig. 3), our results indicate that $g(r)$ is not as sensitive to the structural changes as the diffraction patterns.

A complete halo appears in the diffraction patterns for doses of 0.16 epa and 0.20 dpa. The occurrence of such a complete halo is taken as a sign of amorphization in HVEM experiments. Thus the evidence from the diffraction patterns shows that $NiZr_2$ can be amorphized either by random atom exchanges to a dose of 0.16 epa or Frenkel-pair introduction to 0.2 dpa. This evidence is supported by the [001] atom projections shown in Fig. 7, which indicate progressive structural disorder with dose for both type of defects. The atom projections corresponding to 0.16 epa and 0.2 dpa resemble that of the quenched liquid. It is difficult to exactly pinpoint the onset of amorphization. However, based on the attainment of the quenched liquid level by the energy and volume and the appearance of structural disorder in the atom projections and diffraction patterns, we have determined the onset of amorphization to be around 0.13 dpa and 0.13 epa.

We have also calculated the long-range-order parameter S for various exchange doses below 0.13 epa. For doses in excess of 0.13 epa, lattice sites could not be defined because of significant topological disorder. The long-range-order parameter S is defined as

$$S=\frac{f-r}{1-r}\ , \tag{2}$$

where f is the fraction of a certain atomic species present

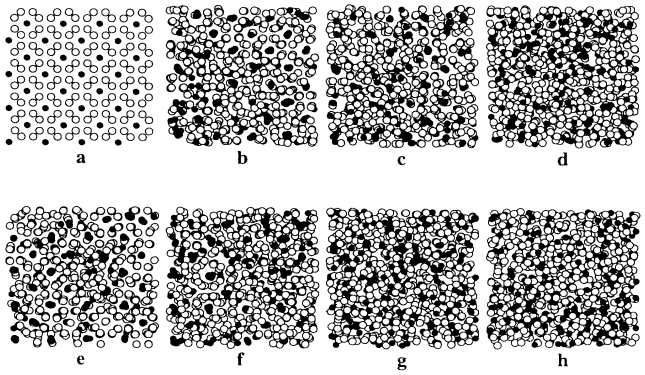

FIG. 7. Projections of atom positions onto the (001) plane corresponding to the following configurations: (a) perfect crystal, (b) 0.07 epa, (c) 0.09 epa, (d) 0.16 epa, (e) 0.07 dpa, (f) 0.13 dpa, (g) 0.2 dpa, and (h) quenched liquid.

on its own lattice site and r is the ratio of the number of atoms of that species to the total number of atoms. The variation of S with dose, prior to the onset of amorphization, is shown in Fig. 8. From the figure, it is apparent that amorphization occurs when S drops below a value of about 0.6. Massobrio, Pontikis, and Martin[10] have also reported amorphization of $NiZr_2$ for $S \leq 0.6$. This observation is consistent with the critical value of $S \approx 0.5$ determined by Xu *et al.*[16] in $NiZr_2$.

C. Mechanical properties

In addition to the structural and thermodynamic properties, the elastic constants of the system can provide valuable information about the crystalline-to-amorphous transition. Okamoto and co-workers[27,28] have pointed out that elastic softening, indicative of a mechanical instability, precedes amorphization by irradiation. In studies of 1-MeV Kr^+ irradiation of Zr_3Al (Refs. 27 and 28) and 1.8-MeV α-particle irradiation of Nb_3Ir,[29] it has been shown that irradiation can bring about a large decrease (about 50%) in the elastic constants. We have determined the elastic constants of $NiZr_2$ using the approach of Ray, Moody, and Rahman.[30] The shear elastic constants C_{44} and C' and their average G are shown in Fig. 9. The constant C_{44} denotes the average of C_{44}, C_{55}, and C_{66}, and C' is defined as

$$C' = \frac{(C_{11}+C_{22}+C_{33})-(C_{12}+C_{23}+C_{13})}{6} . \quad (3)$$

The elastic constants C_{44} and C' decreased with dose following exchanges as well as Frenkel-pair introduction. These constants became equal, indicating the attainment of elastic isotropy, at doses of 0.13 epa and 0.15 dpa. This can be used as an indication of amorphization in a computer simulation. The average shear elastic constant G fell by about 60% of its value in the perfect crystal prior to amorphization. These results are consistent with our observation of an elastic softening prior to amorphization in NiZr (Ref. 14) and the experimental results of Okamoto and co-workers.[27,28] The evidence from the mechanical properties is consistent with that from the structural and thermodynamic properties, and shows that $NiZr_2$ can be amorphized by random atom exchanges or the introduction of Frenkel pairs.

D. Defect-formation energy

The effects of chemical disorder on amorphization of $NiZr_2$ are different from that of CuTi reported by Sabochick and Lam.[11] In an effort to understand this difference, we have calculated the energies of formation of a Frenkel pair and a pair of antisite defects using the approach of Shoemaker *et al.*[31] We have found these values to be 2.75 and 2.17 eV, respectively. The corresponding values in NiZr, which can be amorphized by either defect, are 2.59 and 2.18 eV. In CuTi, which can be amorphized by Frenkel defects but not by antisite defects, Sabochick and Lam[11] have calculated formation energies of 2.79 and 0.38 eV, respectively. Since the antisite defect energy is much larger in NiZr and $NiZr_2$ than in CuTi, chemical disordering can trigger amorphization of NiZr and $NiZr_2$ but not CuTi. The Frenkel-pair energies are quite similar in these compounds, and not surprisingly Frenkel-pair introduction can amorphize all three compounds. It must be pointed out, however, that when a large, nonequilibrium concentration of Frenkel pairs is introduced, most of them recombine and produce chemical disorder.[22] Thus chemical disorder is responsible for

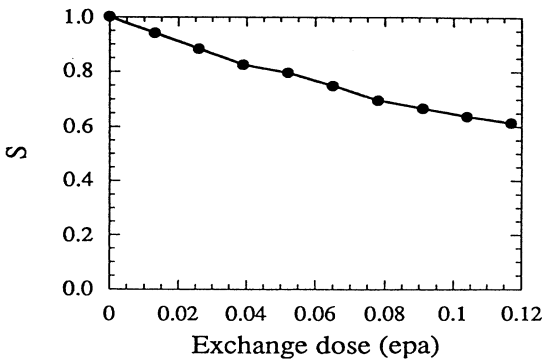

FIG. 8. Long-range-order parameter as a function of exchange dose.

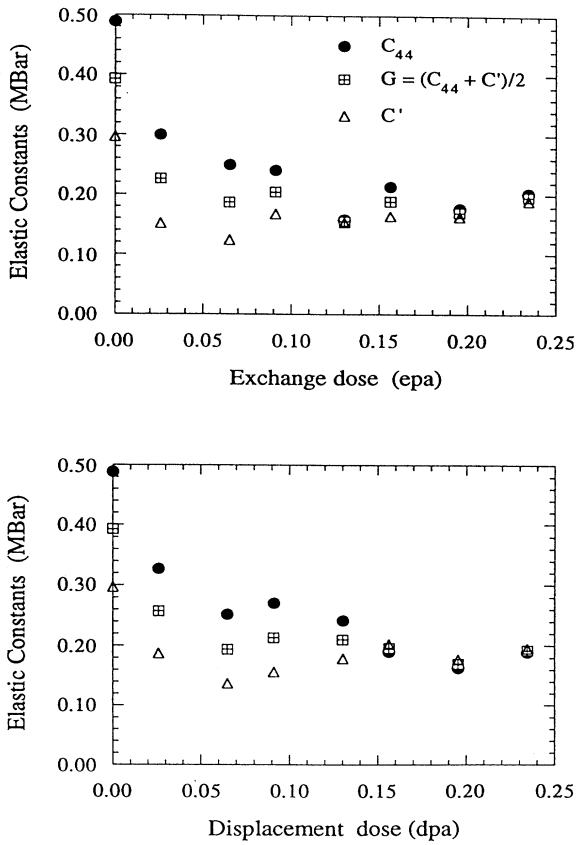

FIG. 9. Shear elastic constants plotted as functions of damage dose following random atom exchanges and Frenkel-pair introduction.

much of the energy increase. In NiZr and $NiZr_2$, this energy increase is sufficient to bring about amorphization. On the other hand, in CuTi it is insufficient, and the survival of Frenkel pairs is essential to complete the crystalline-to-amorphous transition. The ability of chemical disorder to amorphize some compounds and not others indicates that the mechanism of amorphization can vary from compound to compound.

E. Generalized melting criterion

In an effort to account for differences in amorphization tendency among intermetallic compounds, various criteria have been proposed for electron-irradiation-induced amorphization.[9,32–34] These have been based on the crystal structure, electronic structure, ordering energy, solubility range, position of constituents in the periodic table, and the composition ratio of the constituent elements. While the criteria help to illustrate general trends, they are not always dependable. For most of these rules governing amorphization, an exception can be found. Recently, we have proposed a generalization of the Lindemann melting criterion to explain solid-state amorphization.[13,35] In this section we present evidence in favor of this generalized melting criterion.

The original Lindemann melting criterion[36] suggests that an ideal crystal melts when the root-mean-square amplitude of thermal vibrations, $\langle \mu^2_{\rm vib} \rangle^{1/2}$, exceeds a critical value given by $\langle \mu^2_{\rm cri} \rangle^{1/2}$. $\langle \mu^2_{\rm vib} \rangle$ is small compared to $\langle \mu^2_{\rm cri} \rangle$ in the case of radiation-induced amorphization, because it often occurs well below room temperature. However, radiation introduces static atomic displacements via point defects and chemical disorder. By assuming statistical independence of thermal and static displacements,[37] we can define the total displacement $\langle \mu^2_T \rangle$ as the sum of the thermal component $\langle \mu^2_{\rm vib} \rangle$ and the static component $\langle \mu^2_{\rm sta} \rangle$. The Lindemann melting criterion can thus be generalized to include solid-state amorphization as well as melting by applying it to the total displacement instead of just the thermal displacement. According to this generalized melting criterion,[13,35,38] a crystal can be destabilized when the total mean-square atomic displacement $\langle \mu^2_T \rangle$ exceeds the critical value $\langle \mu^2_{\rm cri} \rangle$, i.e.,

$$\langle \mu^2_T \rangle = \langle \mu^2_{\rm sta} \rangle + \langle \mu^2_{\rm vib} \rangle \geq \langle \mu^2_{\rm cri} \rangle \ . \tag{4}$$

For the case of isobaric heating of a perfect crystal, $\langle \mu^2_T \rangle$ is the same as $\langle \mu^2_{\rm vib} \rangle$, while for isothermal disorder (chemical disorder, Frenkel pairs, etc.), $\langle \mu^2_{\rm sta} \rangle$ is the dominant component. In this treatment, no importance is attached to the manner in which the displacement is produced; it is the total magnitude that is significant.

The thermodynamic driving force for the collapse of the crystalline lattice can now be coupled to $\langle \mu^2_T \rangle$ through the Debye temperature. According to the generalized melting criterion, the Debye temperature Θ and the average shear elastic constant G can be related to $\langle \mu^2_T \rangle$ by

$$\frac{\Theta_d^2}{\Theta_c^2} = \frac{G_d}{G_c} = 1 - \frac{\langle \mu_T^2 \rangle}{\langle \mu^2_{\rm cri} \rangle} \ , \tag{5}$$

where the subscripts d and c denote values for the defective and perfect crystals, respectively. Mechanical melting occurs when $\langle \mu^2_T \rangle \rightarrow \langle \mu^2_{\rm cri} \rangle$ such that $\Theta_d \rightarrow 0$ and $G_d \rightarrow 0$. However, G_d does not vanish during solid-state amorphization because the crystal-to-amorphous transition becomes favorable before $\langle \mu^2_T \rangle$ reaches $\langle \mu^2_{\rm cri} \rangle$, i.e., when $\langle \mu^2_T \rangle$ equals $\langle \mu^2_{\rm cri} \rangle^t$. This corresponds to a critical state of disorder when the Debye temperature and average shear elastic constant of the defective crystal become equal to the corresponding quantities of the amorphous state. At this point, the enthalpy difference between the defective crystal and the amorphous state given by[1]

$$\Delta H_{d\text{-}a} = L_d \left[1 - \frac{\Theta_a^2}{\Theta_d^2} \right] \tag{6}$$

vanishes, and amorphization becomes thermodynamically possible. Here, L_d is the heat of fusion of the crystal and the subscript a denotes the amorphous state.

In an effort to verify the generalized melting criterion, we have calculated $\langle \mu^2_T \rangle$ for isobaric heating up to the melting point and for two different isothermal disordering processes, namely, random atom exchanges and Frenkel-pair introduction. The determination of $\langle \mu^2_T \rangle$ is, however, not straightforward for two reasons. First, for the sake of consistency, we have to use the same approach to calculate $\langle \mu^2_T \rangle$ for all three processes. Second, the method of introducing Frenkel pairs into the lattice (moving an atom from its lattice site to an interstitial position away from the original site) leads to large artificial atomic displacements. These displacements should not be considered while calculating the mean-square static displacement. For large concentrations of Frenkel pairs, it is not possible to define lattice sites or to keep track of artificial displacements. To overcome these hurdles, we adopted the following approach to determine $\langle \mu^2_T \rangle$. Let r_{ij} be the distance between an atom i and one of its M first neighbors j. The average first-neighbor distance for atom i is

$$\bar{r}_i = \frac{1}{M} \sum_{j=1}^{M} r_{ij} \ . \tag{7}$$

Let there be N_A atoms of atomic species A and N_B atoms of species B in the system. The variance in $\bar{r}_i$ (i.e., the square of the dispersion in the average nearest-neighbor distance) for A atoms is given by

$$\sigma_A^2 = \frac{1}{N_A} \sum_{i=1}^{N_A} \left[\bar{r}_i - \frac{1}{N_A} \sum_{i=1}^{N_A} \bar{r}_i \right]^2 \ . \tag{8}$$

Similarly, for B atoms we have

$$\sigma_B^2 = \frac{1}{N_B} \sum_{i=1}^{N_B} \left[\bar{r}_i - \frac{1}{N_B} \sum_{i=1}^{N_B} \bar{r}_i \right]^2 \ . \tag{9}$$

The determination of the first-neighbor cutoff distance is not trivial in disordered systems. We defined this cutoff distance as the first minimum in the global pair-correlation function.

In an ideal crystal, both σ_A^2 and σ_B^2 are equal to zero,

because all A atoms lie in a unique first-neighbor environment and so do all B atoms. When atoms are displaced, either by isobaric heating or by isothermal disorder, σ_A^2 and σ_B^2 attain nonzero values. In general, the larger the magnitude of atomic displacements, the larger will be the values of σ_A^2 and σ_B^2. We have verified this for the case of heating by plotting $\langle \mu^2_{\rm vib} \rangle$ as a function of $\sigma^2=(\sigma_A^2+\sigma_B^2)/2$ for temperatures below the melting point as shown in Fig. 10. In the calculation of σ^2, the first-neighbor distance was determined from the position of the first minimum of the pair-correlation function. Figure 10 shows that σ^2 varies linearly with $\langle \mu^2_{\rm vib} \rangle$ for the heating case, indicating that σ^2 can be used as a measure of $\langle \mu^2_T \rangle$.

Figure 11 shows the dependence of the average shear elastic constant G on volume expansion and atomic displacements following isobaric heating up to melting and isothermal disorder (random atom exchanges and Frenkel-pair introduction) leading to amorphization. In Fig. 11(a), G is shown as a function of volume expansion for these processes. One can see that the volume expansions required for melting and amorphization are drastically different, and the two curves have different slopes. The heating of a perfect crystal brings about a homogeneous volume change, while the volume change brought about by isothermal disorder is heterogeneous. It is clear from Fig. 11(a) that volume expansion cannot be a common link between amorphization and melting. Figure 11(b) is a plot of σ^2/σ_M^2 as a function of volume expansion for the two cases. Here, σ^2 has been normalized by its value in the liquid, σ_M^2. Once again the slopes are quite different, indicating that a heterogeneous process can accommodate the same mean-square atomic displacement with a smaller volume expansion than a homogeneous process.

Figure 11(c) is the most interesting of the three subplots. It shows the variation of G with σ^2/σ_M^2. The data points for amorphization (by two different processes) and for melting lie on the same curve. The arrow indicates the datum point corresponding to the solid just below the melting point (1500 K). Upon further heating, there is a big jump in the value of σ^2 and a corresponding sharp drop in G to about zero, and the liquid state is reached. On the other hand, once the system is amorphized, further introduction of defects does not appreciably change σ^2 or G. It is interesting to note that the mean-square atomic displacement is nearly the same prior to melting and amorphization. Moreover, the variation of the average elastic constant with displacement is similar for all three processes and provides support for the generalized melting criterion. The variation of G with σ^2 is also consistent with the calculations of Knuyt and Stals.[39] The results from this work are in agreement with our observations in NiZr, NiTi, and FeTi, where the variation of G with σ^2/σ_M^2 was also found to be similar for isothermal disorder and isobaric heating.[38] In addition, in NiTi and

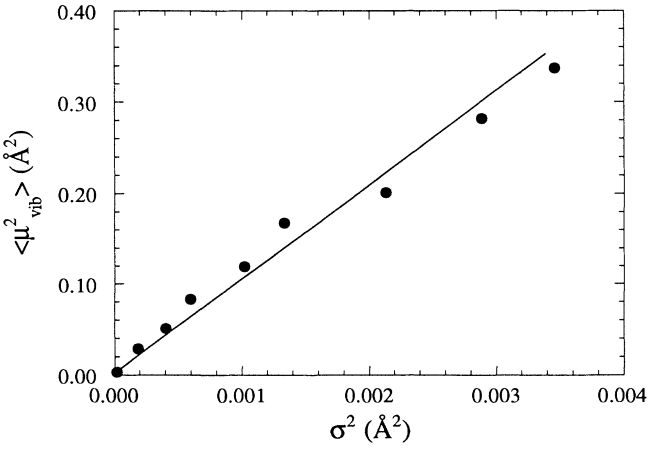

FIG. 10. Variation of the mean-square amplitude of thermal vibrations, $\langle \mu^2_{\rm vib} \rangle$, with the variance σ^2 in average nearest-neighbor distance.

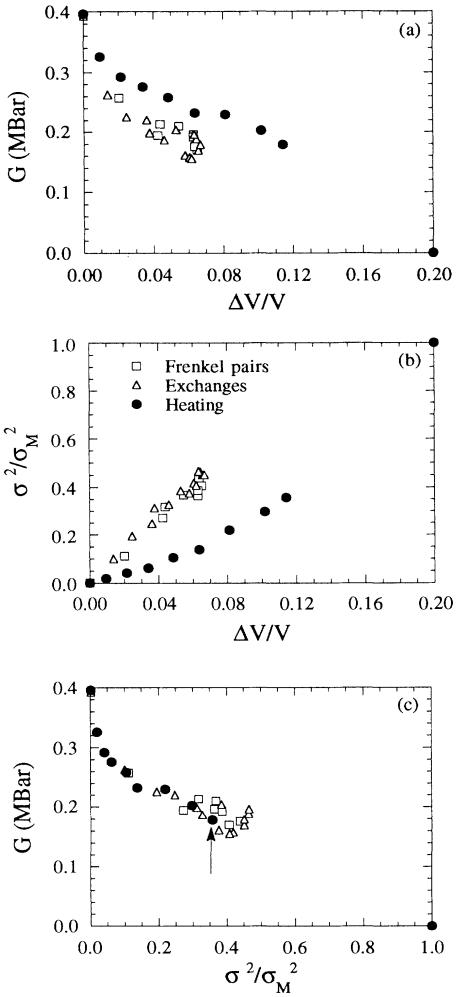

FIG. 11. Effect of isothermal disorder (exchanges and Frenkel pairs) and isobaric heating on $NiZr_2$. (a) The average shear elastic constant G as a function of volume expansion $\Delta V/V$, (b) the normalized variance σ^2/σ_M^2 in average nearest-neighbor distance as a function of $\Delta V/V$, (c) the variation of G with σ^2/σ_M^2. The arrow corresponds to the solid just below its melting point (1500 K).

FeTi, which were not amorphized by chemical disorder, σ^2 and G saturated with dose before reaching the critical values corresponding to the amorphous state.

Further evidence in favor of the generalized melting criterion is provided by the HVEM study of the Ni-Zr system by Xu *et al.*[16] The Debye temperature for compounds of this system in the crystalline and amorphous states have been determined by Kuentzler and co-workers[40,41] and Onn *et al.*,[42] respectively. The Debye-temperature difference between the crystal and glass is smallest for $NiZr_2$ and largest for Ni_3Zr. From our generalized melting criterion [Eq. (6)], it is possible to predict that among the compounds of the Ni-Zr system $NiZr_2$ will be the easiest to amorphize and Ni_3Zr the most difficult. Xu *et al.*[16] irradiated the compounds $NiZr_2$, NiZr, and Ni_3Zr with 1-MeV electrons at 10 K and found that this was indeed the case.

IV. CONCLUSIONS

We have studied electron-irradiation-induced amorphization of $NiZr_2$ using MD simulations in conjunction with embedded-atom potentials. Following Frenkel-pair introduction as well as random atomic exchanges, the energy and volume of the system rose to the levels of the quenched liquid and saturated at those values. The variation of the volume was remarkably similar to that of the energy. The evolution of the system structure was investigated by monitoring the changes in the [001] diffraction patterns calculated using the multislice method in conjunction with the MD trajectories corresponding to various damage doses. Our study suggests that the calculated diffraction patterns are sensitive and reliable probes of the structure of the system. In addition, the pair-correlation functions and atom projections were also determined. It was found that $NiZr_2$ could be amorphized either by Frenkel pairs or by chemical disorder. The long-range-order parameter fell to ~ 0.6 prior to amorphization. Signs of complete amorphization were observed at doses of 0.16 epa and 0.2 dpa. At this point, the average shear elastic constant dropped by about 60% from its value in the perfect crystal, and the material became elastically isotropic. Furthermore, the total mean-square atomic displacement was nearly the same near the melting point and the onset of amorphization. Our findings lend support to the recently proposed generalized melting criterion. The behavior of the shear elastic constants is in agreement with the measurements of elastic softening by Okamoto and co-workers.[27,28] The results of the present simulation are also in good accord with the experimental observations of Xu *et al.*[16] and consistent with the simulation results of Massobrio, Pontikis, and Martin.[10] Our examination of the formation energies of Frenkel and antisite defects provides an explanation for the different effects that chemical disorder has on CuTi and $NiZr_2$.

ACKNOWLEDGMENTS

One of the authors (R.D.) would like to thank Professor L. D. Marks and Dr. M. J. Sabochick for several fruitful discussions. This work was supported by the U.S. Department of Energy, B.E.S. Materials Sciences under Contract No. W-31-109-Eng-38 (N.Q.L., P.R.O.) and the National Science Foundation under Grant No. DMR-8802847 (R.D., M.M.). It has benefited from a grant of time on the Cray computers at NERSC, Lawrence Livermore National Laboratory.

*Corresponding address: Building 212-C224, Argonne National Laboratory, Argonne, Illinois 60439.

[1]P. R. Okamoto and M. Meshii, in *Science of Advanced Materials,* edited by H. Wiedersich and M. Meshii (ASM, Metals Park, OH, 1990).

[2]G. J. C. Carpenter and E. M. Schulson, J. Nucl. Mater. **23**, 180 (1978).

[3]H. Mori and H. Fujita, Jpn. J. Appl. Phys. **21**, L494 (1982).

[4]H. Mori, H. Fujita, and M. Fujita, Jpn. J. Appl. Phys. **22**, L94 (1983).

[5]D. F. Pedraza, J. Mater. Res. **1**, 425 (1986).

[6]Y. Limoge and A. Barbu, Phys. Rev. B **30**, 2212 (1984).

[7]J. Koike, P. R. Okamoto, L. E. Rehn, and M. Meshii, Met. Trans. A **21**, 1799 (1990).

[8]D. E. Luzzi, H. Mori, H. Fujita, and M. Meshii, Scr. Metall. **18**, 957 (1985); Acta Metall. **34**, 629 (1986).

[9]D. E. Luzzi and M. Meshii, Res. Mech. **21**, 207 (1987).

[10]C. Massobrio, V. Pontikis, and G. Martin, Phys. Rev. B **41**, 10 486 (1990).

[11]M. J. Sabochick and N. Q. Lam, Phys. Rev. B **43**, 5243 (1991).

[12]M. J. Sabochick and N. Q. Lam, in *Surface Chemistry and Beam-Solid Interactions,* edited by H. A. Atwater, F. A. Houle, and D. H. Lowndes, Mater. Res. Soc. Symp. Proc. No. 201 (Materials Research Society, Pittsburgh, 1991), p. 387.

[13]N. Q. Lam, P. R. Okamoto, M. J. Sabochick, and R. Devanathan, J. Alloys Compounds (to be published).

[14]R. Devanathan, N. Q. Lam, M. J. Sabochick, P. R. Okamoto, and M. Meshii, J. Alloys Compounds (to be published).

[15]R. Devanathan, N. Q. Lam, M. J. Sabochick, P. R. Okamoto, and M. Meshii, in *Phase Formation and Modification by Beam-Solid Interactions,* edited by G. S. Was, L. E. Rehn, and D. M. Follstaedt, Mater. Res. Soc. Symp. Proc. No. 235 (Materials Research Society, Pittsburgh, 1992), p. 539.

[16]G. Xu, M. Meshii, P. R. Okamoto, and L. E. Rehn, J. Alloys Compounds (to be published).

[17]M. S. Daw, M. I. Baskes, and S. M. Foiles (private communication).

[18]D. J. Oh and R. A. Johnson, J. Mater. Res. **3**, 471 (1988).

[19]M. S. Daw and M. I. Baskes, Phys. Rev. B **29**, 6443 (1984).

[20]F. R. Eshelman and J. F. Smith, J. Appl. Phys. **46**, 5080 (1975).

[21]P. Nash and C. S. Jayanth, Bull. Alloy Phase Diagrams **5**, 144 (1984).

[22]R. Devanathan, N. Q. Lam, M. J. Sabochick, P. R. Okamoto, and M. Meshii, in *Defects in Materials,* edited by P. D. Bristowe, J. E. Epperson, G. E. Griffith, and Z. Lilienthal-Weber, Mater. Res. Soc. Symp. Proc. No. 209 (Materials Research Society, Pittsburgh, 1991), p. 231.

[23]J. M. Cowley and A. F. Moodie, Acta Crystallogr. **10**, 609 (1957); **12**, 353 (1959); **12**, 60 (1959).
[24]K. Ishizuka and N. Uyeda, Acta Crystallogr. A **33**, 740 (1977).
[25]P. G. Self and M. A. O'Keefe, in *High Resolution Transmission Electron Microscopy and Associated Techniques,* edited by P. R. Buseck, J. M. Cowley, and L. Eyring (Oxford University Press, New York, 1988).
[26]R. Devanathan, N. Q. Lam, P. R. Okamoto, and M. Meshii (unpublished).
[27]P. R. Okamoto, L. E. Rehn, J. Pearson, R. Bhadra, and M. Grimsditch, J. Less-Common Met. **140**, 231 (1988).
[28]L. E. Rehn, P. R. Okamoto, J. Pearson, R. Bhadra, and M. Grimsditch, Phys. Rev. Lett. **59**, 2987 (1987).
[29]M. Grimsditch, K. E. Gray, R. Bhadra, R. T. Kampwirth, and L. E. Rehn, Phys. Rev. B **35**, 883 (1987).
[30]J. R. Ray, M. C. Moody, and A. Rahman, Phys. Rev. B **32**, 733 (1985); **33**, 895 (1986).
[31]J. R. Schoemaker, R. T. Lutton, D. Wesley, W. R. Wharton, M. L. Oehrli, M. S. Herte, M. J. Sabochick, and N. Q. Lam, J. Mater. Res. **6**, 473 (1991).
[32]J. L. Brimhall, H. E. Kissinger, and L. A. Charlot, Radiat. Eff. **77**, 273 (1983).
[33]H. Mori, H. Fujita, M. Tendor, and M. Fujita, Scr. Metall. **18**, 783 (1984).
[34]A. Bieber and F. Gautier, Solid State Commun. **38**, 1219 (1981).
[35]N. Q. Lam, P. R. Okamoto, R. Devanathan, and M. Meshii, in Proceedings of the NATO Advanced Study Institute on Statistics and Dynamics of Alloy Phase Transformations, Rhodes, Greece, 1992 (Plenum, New York, in press).
[36]A. Lindemann, Z. Phys. **11**, 609 (1910).
[37]A. Voronel, S. Rabinovich, A. Kisliuk, V. Steinberg, and T. Sverbilova, Phys. Rev. Lett. **60**, 2402 (1988).
[38]R. Devanathan, N. Q. Lam, P. R. Okamoto, and M. Meshii, in *Materials Theory and Modeling,* edited by P. D. Bristowe, J. Broughton, and J. M. Newsam, Mater. Res. Soc. Symp. Proc. No. 291 (Materials Research Society, Pittsburgh, in press).
[39]G. Knuyt and L. M. Stals, Philos. Mag. B **64**, 299 (1991).
[40]R. Kuentzler, J. Phys. F **14**, L79 (1984).
[41]A. Amamou, R. Kuentzler, Y. Dossmann, P. Forey, J. L. Glimois, and J. L. Feron, J. Phys. F **12**, 2509 (1982).
[42]D. G. Onn, L. Q. Wang, Y. Obi, and K. Fukamichi, Solid State Commun. **46**, 37 (1983).